Investigation of Thermohydraulic Performance of Multiple Tube Pass Heat Exchanger with Baffles

Muhammad Ali Kamran[*], Muhammad Alam Zaib Khan[†], Zahid Hussain Shah[‡], Usman Jadoon[§], Shayan Javed[**], Adil Shareen[††]

Abstract

Shell side design and analysis of a small shell and tube heat exchanger with baffles and two tube passes is reported. The effect of different baffle spacing on parameters such as heat transfer, Number of Transfer units (NTU) and pressure drops was studied using numerical and experimental techniques to identify the inter baffle spacing for optimal thermohydraulic performance. Contrary to earlier studies in this area, both the shell and tube fluids along with channels were modeled for multiple tube passes; besides conduction effects along the baffle were also considered. Segmented baffles with a baffle cut of 20% were simulated in ANSYS for multiple inlet temperatures. Turbulence was modeled using the realizable k-ε scheme while the Bell-Delaware method was employed for pressure drops. Increase in heat transfer was observed when the number of baffles was increased, but an inter baffle spacing ratio of 0.41 was identified to be the optimal for thermohydraulic performance. Experimental investigation conducted to gauge the reliability of the results displayed a close match showing that the current numerical methodology can be used to design and assess industrial heat exchangers with segmented baffles and multiple tube passes.

Keywords: Multiple tube passes, Segmented baffles, Heat exchangers, Baffle Spacing, Computational

Introduction

Heat exchangers (HXs) are devices that facilitate exchange of heat between two fluids which are at different temperatures without mixing (Cengel, 2003). They help regulate the fluid temperatures for different applications besides working as heat recovery devices, leading to energy conservation. Various types of HXs are in use commercially with the shell and tube (ST) type the most and commonly used basic HX. These are in wide use in the manufacturing industry, thermal power plants and energy

[*] Corresponding & First author, Department of Mechanical Engineering, University of Engineering and Technology, Peshawar 25120, Pakistan, alikamran@uetpeshawar.edu.pk
[†] Department of Mechanical Engineering, University of Engineering and Technology, Peshawar 25120, Pakistan, alamzaibkhan@uetpeshawar.edu.pk
[‡] Department of Mechanical Engineering, University of Engineering and Technology, Peshawar 25120, Pakistan, zahid3325@outlook.com
[§] Department of Mechanical Engineering, University of Engineering and Technology, Peshawar 25120, Pakistan, usman.jadoon@outlook.com
[**] Department of Mechanical Engineering, University of Engineering and Technology, Peshawar 25120, Pakistan, shayanjaved@gmail.com
[††] Department of Mechanical Engineering, University of Engineering and Technology, Peshawar 25120, Pakistan, engr.adilshareen@gmail.com

conservation systems. Due to their simplistic structure, more than 35% of HXs are ST type (Master, Chunangad, & Pushpanathan, 2003)**.** Baffles are one of the key components of HXs which provide structural support to the tubes and increase the HX effectiveness (Kakac & Hongtan, 2000). The complex circulation of the fluid makes the design of HXs complex. Traditionally, the HX design has been an iterative process with a standardized design tested and improved if performance was not found up to the mark. This was a costly process; with the advent of high speed computers and development of CFD methodologies, the prototypes are made virtually (Sunden, 2007).

Different approaches towards numerical modeling of HXs have been reported in the literature such as the porous concept, periodic model and unit channel model (Yang, Ma, Bock, Jacobi, & Liu, 2014; Prithiviraj & Andrews, 1998). However, the full model approach is recommended since it gives the best results (Ozden & Tari, 2010; Wang, Chen, Chen, & Zing, Numerical InvestIgation on Combine Multiple Shell-Pass Shell and Tube Heat Exchanger wih Continuous Helical Baffles, 2009). Bell Delaware (Cao, 2010) and Kern (Cao, 2010) are empirical methods which serve as a good design reference for STHXs.

Different baffle geometries such as double segmental baffles (Williams & Knudsen, 1963), rod baffle (Xianhe & Songjiu, 1998), ring baffles (You, Fan, Liu, & Huang, 2012), etc. have been proposed as a replacement to segmented baffles. However, segmented baffles, which have a cut that allows the fluid to pass through are the most widely used baffle type (Kottke, 1999) due to their flexible assembly (Liu, 2015).

Performance of the HX is affected by the baffle cut, measured as a percent of the baffle diameter, and the distance between successive baffles. Computational analysis is the most popular research tool used for optimizing the design parameters of segmented baffle. Ozden and Tari (Ozden & Tari, 2010) carried out numerical simulations of only the shell side of a small HX with a single pass to compare the predictions of 3 different turbulence models (Spalart-Allmaras, standard and realizable k-ε models). Segmental baffles with cuts of 25% and 36% were simulated, and the effect of baffle spacing was studied. Predictions from the realizable k-ε model were found to be in good agreement with the Bell-Delaware method. Similar to Mukherjee (Mukherjee, 1998), the optimum value for the baffle spacing to shell diameter ratio was proposed to be in the range of 0.3 to 0.6. A drawback of this investigation was that flow inside the tubes was not considered, and tubes were treated as isothermal walls. Wang (Wang, Chen, Chen, & Zing, Numerical Investigation on

Combine Multiple Shell-Pass Shell and Tube Heat Exchanger wih Continuous Helical Baffles, 2009) modeled a two tube pass HX employing the realizable k-ε model using different baffle types in the shells. The study was a continuation to Andrews (Andrews & Master, 2005) who analyzed a HX with continuous helical baffles, concluding those to be better than segmental baffles at enhancing the heat transfer rate.

Stehlik et al. (Stehlik, Nemcansky, Kral, & Swanson, 1994) also performed CFD comparison of helical baffles and segmental baffles; heat transfer and pressure drops showed a considerable advantage on the shell side with helical baffles. Although the helical baffles were better at increasing the heat transfer rate in (Andrews & Master, 2005; Stehlik, Nemcansky, Kral, & Swanson, 1994) segmental baffles have the inherent advantage of being simple in manufacturing and design; hence they are more feasible. Another baffle type that has found some interest recently is the use of plate baffles. Plate baffles have slots around tubes, which allow parallel flow over tubes resulting in lesser vibrations and reduced fouling. Yang and Liu (Yang & Liu, Numerical investigation on a novel shell and tube heat exchanger with plate baffles and experimental validation, 2015) compared the performance of plate and rod baffles in a STHX, and reported Nusselt number for plate baffles to be higher than that of rod baffles, resulting in heat transfer increase of up to 15%, albeit with a higher pressure drop. Instead of using continuous slots, Yonghua et al. (Yonghua, et al., 2015) investigated the effect of trefoil holes around tubes in a STHX. These holes induced jets resulting in increased turbulence, hence an increase in heat transfer. Comparison of the predictions made using the standard k-ε model with analytical solutions showed reasonable agreement. Significant local pressure drops were observed as the fluid passed through the trefoil holes.

Insertion of trefoil holes over inclined segmental baffles by Sun et al. (Sun Y, 2019) although reduced the pressure drop but also resulted in a decrease in the heat transfer coefficient. Jozaei et al. (Jozaei, Baheri, Hafshejani, Arad, & Falavan, 2012) worked on the optimization of baffle spacing on heat transfer, pressure drop and overall cost of the HX. Reduction in pressure drop and heat transfer was reported with an increase of baffle spacing. However, the pressure drop was not affected beyond certain baffle spacing, although heat transfer continued to be affected with further increase in baffle spacing.

The discussion above has summarized various baffle types that are being investigated currently. The objective of testing the different devices was to identify the optimum balance between enhanced heat transfer, drop

in pressure and ease of usage. Although much work has been done on segmented baffles in single pass HXs, numerical modeling of multiple pass HXs has been scarce. It is therefore important to investigate the effect of baffle spacing and baffle cut, which are critical parameters affecting the effectiveness of segmental baffles in multiple pass HXs. In this study, effects of baffle spacing on heat transfer and pressure drop are analyzed at a fixed baffle cut of 20% for a small STHX with two tube passes. A simplification adopted in most of the available literature is the use of isothermal tube walls. This reduces the need to simulate the tube flow but has the inherent flaw of over predicting the heat transfer rates since the tube flow is treated as a source (temperature changes in the tube fluid are not considered). In the work reported here, both the tube and shell fluids were modeled to improve the quality of simulations along with conduction across the baffles and tube sheets.

In addition to the numerical investigation, an experimental study on a small STHX is also reported here. Details of the numerical methodology adopted are presented next.

Methodology

3D model of the HX consisting of a single shell with five tubes, each undergoing two tube passes created using PTC Creo 3.0 is shown in Fig. 1. To reduce the computational overhead, use of symmetry was made and only 180° sector of the HX was modeled. The shell, which was assumed adiabatic had an inner diameter of 304.8mm, while the inlet dia of tubes was 16.05mm. Complete details of the HX investigated are given in Table-I.

Unstructured 3D tetrahedral mesh of the complete geometry including the channels was generated using ICEM CFD. Since the accuracy of any CFD simulation depends on the quality of mesh (Sunden, 2007), the mesh density in regions of high velocity and temperature gradients was maximized to obtain the best balance between accurate results and computational overhead. In addition, use of prism layers was made to capture boundary layer flows. An investigation of mesh independence revealed that 5 to 6 million cells were sufficient for the cases investigated. Pal et al. (Pal, Kumar, Joshi, & Maheshwari, 2016) argued that HX simulations are very sensitive to outlet boundary conditions and mesh quality. Separate geometries were created for each case tested, but great care was taken to ensure that the mesh quality remained similar for all the cases. This level of detail was required to ensure that all results were reliable, and there were no outliers as reported in (Ozden & Tari, 2010).

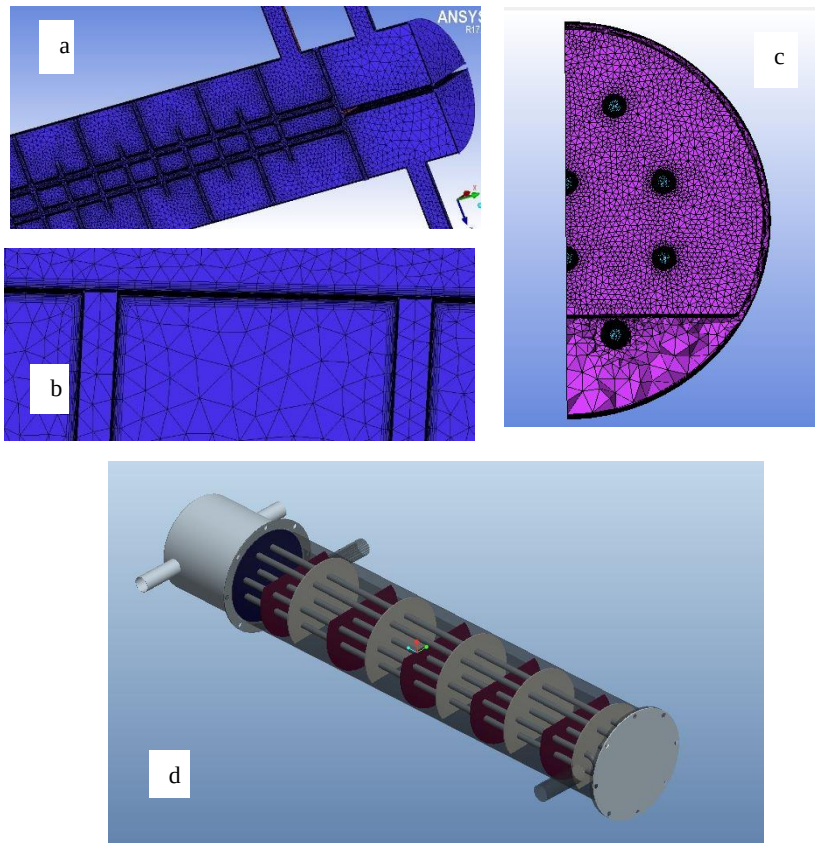

Fig. 1. HX Mesh a) Complete HX b) hybrid mesh with prism layers c) Cross section d) Complete HX with baffles

Table 1
Geometric Dimension and Parameters

Shell inside diameter, d_s	**304.8mm**
Tube inside diameter, d_t	16.05mm
Shell length, l_s	1498mm
Tube length, l_t	1422mm
No. Of tubes, n_t	5
No. Of tube passes, n_p	2
No. Of baffles, n_b	4, 6, 8, 10, 12, 14, 16
Percentage baffle cut, b_s	20

The geometry had two fluid domains, one each for tube fluid and shell fluid. To model conduction in the solid regions, two solid domains

were also created for tube sheets and the baffles (thermal conductivity = 400W/mK). A single segmental baffle with a cut of 20% was used in the study reported here. Maximum inter baffle spacing of less than one shell diameter recommended in (Mukherjee, 1998) meant that the minimum number of baffles required were 6. However, an additional test case with four baffles deemed sufficient to support the tube bundles was also simulated.

CFD predictions for the flowfield were carried out in FLUENT using ANSYS Workbench. Hot fluid at an inlet temperature of 333K was made to flow in the channel head and tubes while the shell inlet temperature was 290K. To reduce the effect of application of boundary conditions on the solution, sections of the inlet tubes were also modeled (see Fig. 1), and constant mass flow rate of 0.1kg/s and 0.2 kg/s was provided to the ST sides respectively. Water with constant thermophysical properties (specific heat = 4180J/kgK, thermal conductivity = 0.64W/mK) was used on either side, and a steady state analysis was performed. Since the primary objective of this study was to determine the effective overall heat transfer coefficients in the presence of baffles, another set of simulations at a higher inlet temperature of 383K was also investigated. The purpose of this simulation-set was to ensure that the changing trends noted in the earlier study are due to the baffles alone, and not due to the decreasing temperature difference between the hot and cold fluids.

Two equation realizable k-ε model with standard wall functions was employed for modeling turbulence. The choice of this model was influenced by (Yang, Ma, Bock, Jacobi, & Liu, 2014; Ozden & Tari, 2010; Jain, Jain, & Patel, 2015) which have identified this model to be most accurate in predicting the heat transfer and pressure losses in HXs. Since the inlet conditions were set at a distance to allow the flow to develop 'naturally', turbulence intensity and turbulence viscosity ratios were set values of 5% and 10 respectively**.**

Table 2
Inlet and Outlet Boundary Conditions

Tube inlet temperature, t_{hi}	333k
Shell inlet temperature, t_{ci}	290k
Tube side mass flow rate, m_h	0.1kg/s
Shell side mass flow rate, m_c	0.2kg/s
Tube side mass flow rate (complete HX)	0.2kg/s
Shell side mass flow rate (complete HX)	0.4kg/s
Outlet Boundary condition (gage pressure)	0 bar

Governing Equations:

Governing equations used by Fluent and employed in this study are summarized below. Since a steady state analysis was performed, the equations have been adapted accordingly.

Continuity: $$\nabla.\left(\rho\vec{V}\right) = 0 \quad (1)$$

x-momentum: $$\nabla.\left(\rho u\vec{V}\right) = -\frac{\partial p}{\partial x} + \frac{\partial \tau_{xx}}{\partial x} + \frac{\partial \tau_{xy}}{\partial y} + \frac{\partial \tau_{zx}}{\partial z} \quad (2)$$

y-momentum: $$\nabla.\left(\rho v\vec{V}\right) = -\frac{\partial p}{\partial y} + \frac{\partial \tau_{xy}}{\partial x} + \frac{\partial \tau_{yy}}{\partial y} + \frac{\partial \tau_{zy}}{\partial z} \quad (3)$$

z-momentum: $$\nabla.\left(\rho w\vec{V}\right) = -\frac{\partial p}{\partial z} + \frac{\partial \tau_{xz}}{\partial x} + \frac{\partial \tau_{yz}}{\partial y} + \frac{\partial \tau_{zz}}{\partial z} + \rho g \quad (4)$$

Energy: $$\nabla.\left(\rho e\vec{V}\right) = -p\nabla.\vec{V} + \nabla.(k\nabla T) + q + \phi \quad (5)$$

where the dissipation function ϕ is calculated using as

$$\phi = \mu\left[2\left[\left(\frac{\partial u}{\partial x}\right)^2 + \left(\frac{\partial v}{\partial y}\right)^2 + \left(\frac{w}{\partial z}\right)^2\right] + \left(\frac{\partial u}{\partial y} + \frac{\partial v}{\partial x}\right)^2 + \left(\frac{\partial u}{\partial z} + \frac{\partial w}{\partial x}\right)^2 + \left(\frac{\partial v}{\partial z} + \frac{\partial w}{\partial y}\right)^2\right] + \lambda\left(\nabla.\vec{V}\right)^2 \quad (6)$$

The set of equations were closed using the transport equations for k and ε (Ansys fluent theory guide, n.d.).

$$\frac{\partial}{\partial t}(\rho k) + \frac{\partial}{\partial x_j}\left(\rho k u_j\right) = \frac{\partial}{\partial x_j}\left[\left(\mu + \frac{\mu_t}{\sigma_k}\right)\frac{\partial k}{\partial x_j}\right] + G_k + G_b - \rho\varepsilon - Y_M + S_k \quad (7)$$

and

$$\frac{\partial}{\partial t}(\rho\varepsilon) + \frac{\partial}{\partial x_j}\left(\rho\varepsilon u_j\right) = \frac{\partial}{\partial x_j}\left[\left(\mu + \frac{\mu_t}{\sigma_\varepsilon}\right)\frac{\partial \varepsilon}{\partial x_j}\right] + \rho C_1 S\varepsilon - \rho C_2 \frac{\varepsilon^2}{k + \sqrt{\nu\varepsilon}} + C_{1\varepsilon}\frac{\varepsilon}{k}C_{3\varepsilon}G_b + S_\varepsilon \quad (8)$$

where eddy viscosity is given as

$$u_t = \rho C_\mu \frac{k^2}{\varepsilon} \quad (9)$$

All model constants have been given conventional values summarized in Table 3.

Table 3
Constants used in transport equations for k and ε

$C_{1\varepsilon}$	C_2	σ_k	σ_ε
1.44	1.9	1.0	1.2

The equations were solved using the pressure based algorithm SIMPLEC due to its faster convergence rates and lower memory requirement (Biswas & Eswaran, 2002) by application of second order upwind scheme. However, to reduce the computational time, the solution was initiated using a first order scheme. Convergence of the solution was established by monitoring the residuals as well as comparison of the results after a fixed number of iterations across the solution domain.

Calculation of Overall Heat Transfer Coefficient U:

The U value**,** which has been used as a basis of comparing the effect of baffle on heat transfer was calculated by employing the ε-NTU method (Bergman, Lavine, Incropera, & Dewitt, 2011).

$$NTU = f(\varepsilon, \frac{C_{min}}{C_{max}})$$

where **ε** is the effectiveness, while C_{min} and C_{max} are the heat capacities of minimum and maximum fluids respectively. Important relationships used in this method are listed below for reference. For further details, the readers can refer to (Bergman, Lavine, Incropera, & Dewitt, 2011)

$$\varepsilon = \frac{Actual\ heat\ transfered}{Maximum\ possible\ heat\ transfer} = \frac{q}{q_{max}}$$

$$q_{max} = C_{min}(T_{hi} - T_{ho}) \quad (9)$$

$$q = m_h c_p (T_{hi} - T_{ho}) = m_c c_p (T_{co} - T_{ci}) \quad (10)$$

Knowing the value of effectiveness and heat capacity rates, NTU was calculated and overall heat transfer coefficient determined as

$$U = \frac{NTU.C_{min}}{A} \quad (11)$$

Experimental Setup:

The experimental investigation was conducted using a HX with a shell of length 800mm and an inlet diameter of 152.4mm. 6 Aluminum tubes of 9mm internal diameter, each undergoing two tube passes carried the hot fluid across the shell. K type thermocouples were installed to determine temperatures of the fluids at inlet and outlet, while mass flow

of the fluids were calculated through volume flow readings. Although the dimensions and inlet conditions of the fluids did not replicate the modeled HX, the results were a good indicator of the validity or otherwise of the numerical methodology employed to study the effect of baffle spacing on heat exchanged. Hot fluid at 346K with a variation of ±1K was supplied from a geyser, while cold fluid supply came from a storage tank at 310K. The temperature readings were measured after attainment of steady state within the HX. Similar to the numerical investigation, a single segmental baffle with a cut of 20% was used, while number of baffles investigated varied from 4 to 14 with an increment of 2.

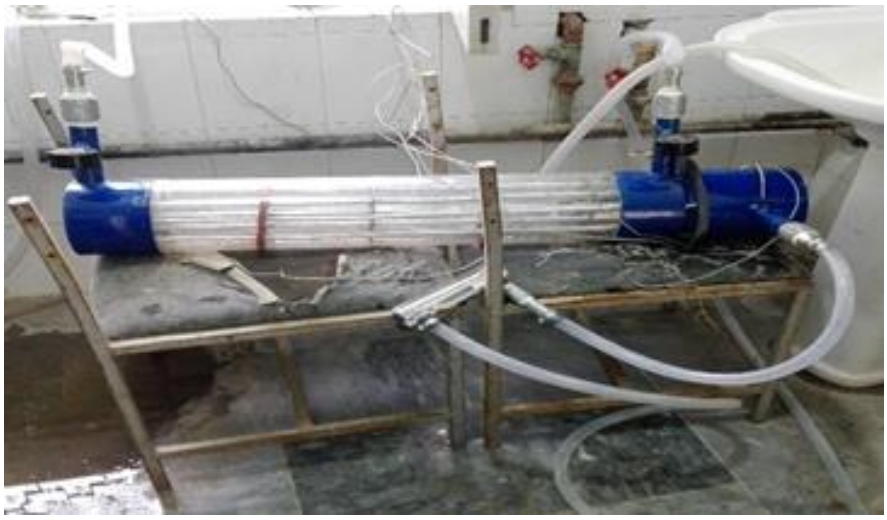

Fig. 2. Experimental setup used for validation of the numerical methodology

Results and discussion

Numerical Simulations

To study the effect of baffle spacing on heat transfer and shell side pressure drops, the number of baffles across the shell was increased from 4-16 with an increment of 2, and its effect on heat transfer and pressure drop was observed. Location of the first baffle was not altered to ensure that the entry region is not disturbed. Thus any changes in the flow field were due to the number of baffles alone.

Effect of baffles on heat transfer and overall heat transfer coefficient

Temperature contours at the symmetry plane of the HX for all the baffle configurations analyzed are shown in Fig. 3. With 6 baffles, the

temperature of the tube fluid (hot, minimum fluid) remains approximately the same throughout, due to very little thermal contact with the shell fluid.

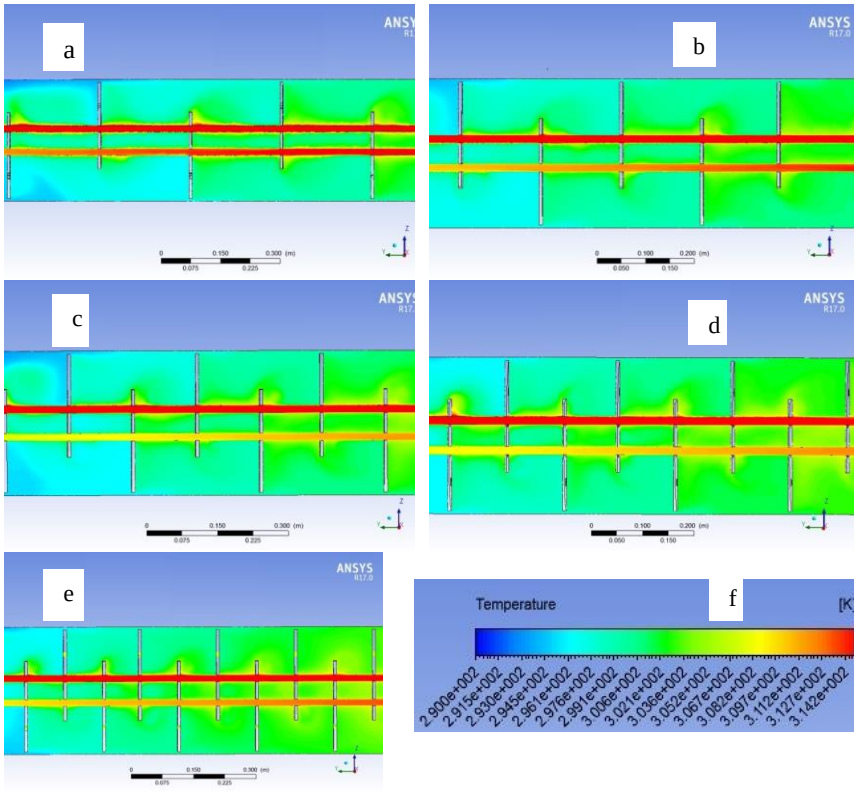

Fig. 3. Temperature Contours at the symmetry plane for different number of baffles a) N=6, b) N=8, c) N=10, d) N=12, e) N=14, f) Temperature legend

The cold fluid gains energy only in regions close to the baffles, but this thermal contact vanishes before the arrival of the next baffle hindrance. As the number of baffles is increased (Figs. 3a and 3b), heat transfer increases, which can be gauged by looking at the temperature changes at the tube outlet (the lower tube pass). Temperature distribution in the shell close to the baffles looks very similar to the earlier case, but the increase in number has made the shell fluid to come in greater contact with the tube walls. As the number is further increased to 10 and 12 (Figs. 3c and 3d), heat transfer rates are enhanced further. Despite the fact that changes are being made on the shell side, the effects are more pronounced

on the tube side due to the lower heat capacity of the hot fluid. A glance at Fig. 3 would also reveal that temperatures at the shell side start getting uniform as the baffle number is increased. Effect of the baffle number beyond 12 on heat transfer cannot be evaluated accurately from the temperature contours, since the temperature contours do not change significantly implying that the baffle spacing has reached an optimum limit.

The enhanced heat transfer observed was due to the changes induced in the flow patterns caused by the introduction of baffles. To explain this, stream traces of the shell fluid at the symmetry plane are shown in Fig. 4. Baffles influence the cross flow stream resulting in creation of recirculation zones within the shell. With 6 baffles, acceleration of the fluid across the baffles created large separation zones leading to lower utilization of the space behind the baffles. The fluid in these zones gets trapped between the solid baffle boundary on one side and the accelerating fluid on the other; lower temperature in this region signify lesser localized heat transfer. By increasing the number of baffles, these recirculation zones are reduced, increasing the effective area of heat transfer within the HX. Reduction in the inter baffle spacing also resulted in an increase in cross flow velocity induced by the baffles, which is more effective than the axial flow for heat transfer. Also notable in Fig. 4 is that as the fluid moves along the shell, the region of separation decreases due to loss of momentum of the fluid which also assists heat transfer. Further elaboration of this phenomenon is depicted in Fig. 5, where temperature contours along the cross section of the HX are shown midway between two baffles. It is evident that as the number of baffles increases, they affect a larger area of the HX, leading to uniform temperature distribution as well as enhanced heat transfer rate.

Table 4

Effect of Inter Baffle Spacing on Heat Transfer (Channel Inlet Temperature 333K)

No. of baffles	B/D_S	Channel outlet temperature (K)	Heat exchanged (kW)	% Increase in heat transfer
4	1.26	311	18.34	--
6	0.72	309.5	19.6	6.87
8	0.54	307.4	21.38	16.57
10	0.41	305.4	23.01	25.45
12	0.33	304.7	23.58	28.53
14	0.28	304.6	23.69	29.16
16	0.24	304.5	23.82	29.88

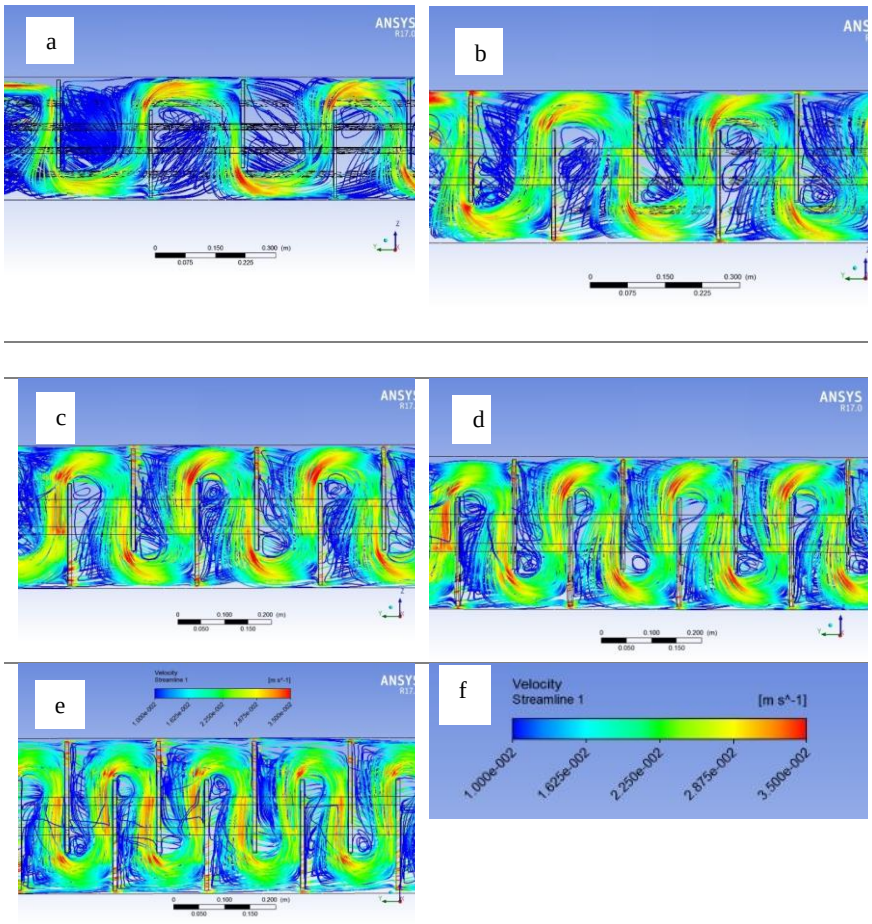

Fig. 4. Stream traces of velocity at the symmetry plane for different number of baffles a) N=6, b) N=8, c) N=10, d) N=12, e) N=14, f) Velocity legend

To identify the optimum number of baffles, a plot of heat transfer against the number of baffles is shown in Fig. 6 and results summarized in Table 4. Increase in heat transfer with an increase in the baffles as discussed above is clearly visible. A significant increase can be seen up to 10 baffles, after which the enhancement in heat transfer diminishes (Table 4). Although, 12 baffles show an increase in heat transfer over 10 baffles, the diminishing return suggests 10 baffles to be more effective. A similar but vivid trend can also be seen in the NTU behavior shown in Fig. 9, clearly indicating 10 baffles to be the optimal number for the baffle cut

investigated in the present study. This corresponds to an inter baffle spacing to shell diameter ratio (B/D_s) of 0.41. This identified optimum falls in the B/D_s range of 0.3-0.6 quoted in (Ozden & Tari, 2010), (Mukherjee, 1998) for single pass HXs.

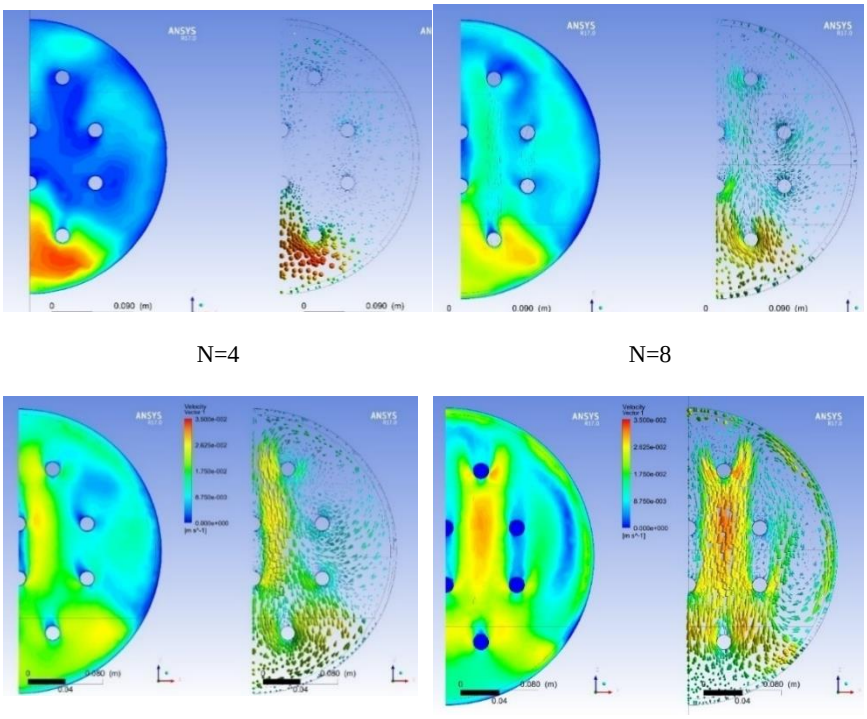

N=4 N=8

N=12 N=16

Fig. 5. Cross Sectional view of the HX for different baffle numbers

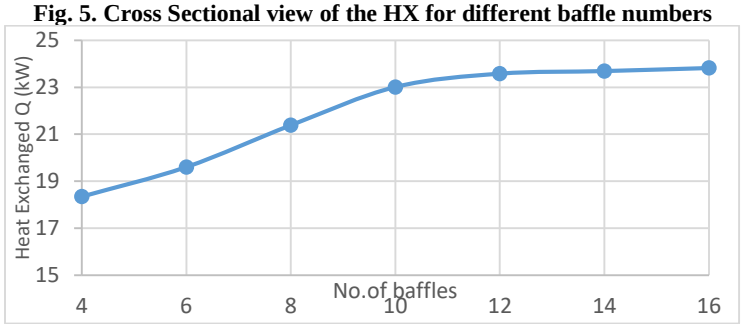

Fig. 6. Effect of number of baffles on heat transfer rate within the HX (channel inlet temperature = 333K)

Since heat transfer in a HX is due to temperature difference between the fluids, the inability of the baffles at enhancing the heat transfer could have been due to the decreasing temperature difference between cold and hot side i.e. the difference has reduced to a level that does not allow further enhancement in heat transfer. To investigate this, another set of simulations was also performed with the same parameters except a higher inlet temperature of the hot fluid (383K). A comparison of the % increase in heat transfer relative to the 4 baffle case at the two different temperatures with varying baffles is presented in Fig. 7. It is evident from the graph that introduction of baffles had the same effect on heat transfer at both the inlet temperatures, signifying that selection of the relatively lower inlet temperature of 333K for the simulations to be adequate for the investigation reported here, and a B/D_s of 0.41 was the optimal value from heat transfer perspective. Hence the overall heat transfer coefficient patterns shown in Fig. 6 are a direct indicator of the effect of baffles on the convection heat transfer on shell side of the HX.

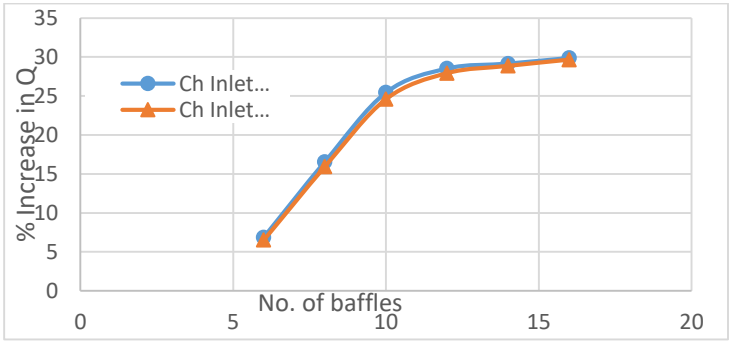

Fig. 7. Percent increase in heat transfer with baffles at different channel inlet temperatures (datum: 4 baffles)

Effects of baffles on pressure drops on shell sides

Two methods, namely the Kern Method (Kern, 1997) and Bell–Delaware Method (Bell, 1963) are generally accepted for determining the heat transfer and pressure drop in STHXs. The Kern method assumes a baffle cut of 25% which is different from the 20% cut used in the current investigation, therefore, the Bell–Delaware method has been employed in the present study to evaluate the thermohydraulic performance of the HX with varying baffles. The shell side pressure drop is the sum of pressure drops for the internal cross-flow sections, the window sections, and the inlet and outlet sections. As expected, an increase in pressure drop with the increasing number of baffles was observed, with the drops more notable beyond 10 baffles.

To gauge the thermohydraulic performance, the ratio of change in pressure drop and increase in heat transfer relative to the 4 baffles case is shown in Fig. 6. An increase in the values exhibits reduced performance. Since the pressure continues to drop parabolically with an increase in number of baffles with little increase in the heat transfer rates beyond 10 baffles, the graph confirms the use of 10 baffles for optimal thermohydraulic performance. With fewer number of baffles, most of distance from shell inlet to outlet is covered longitudinally i.e. parallel to the tube bundle, with very little cross flow component (Fig. 4). As the number is increased, a significant component of the fluid undergoes a direction change across the baffles, which results in pressure drop. These sudden directional changes across the baffles increase the effective length of the HX, which although increases the heat transfer rate but cause a drop in pressure. Hence, the increase in pressure drops is caused by both, an increase in the cross flow velocity and increase in length of the flow path.

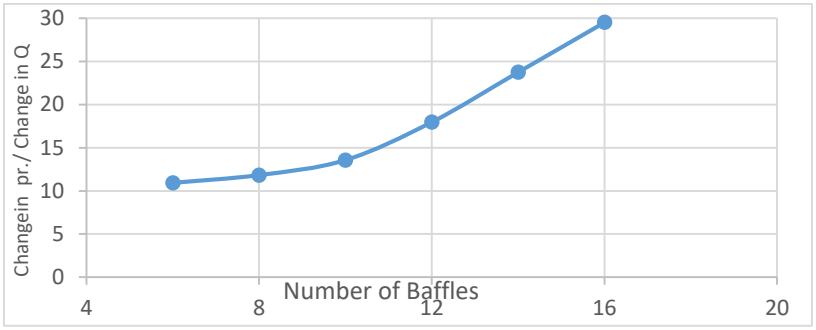

Fig. 8. Effect of Number of baffles on Thermohydraulic performance (Datum: 4 baffles)

Experimental Validation

Summary of the different number of baffles along with the B/Ds ratio tested experimentally is given in Table 5. The purpose of presenting the comparison here is to establish if the methodology adopted for the numerical investigation was able to predict the effect of changing baffles on the heat transfer rate. Although the HX used in the experiments was different from the one numerically modeled, the comparison is presented in non-dimensional terms through B/D_s ratio (Fig. 9). The trends of change in the heat transfer coefficient with the different baffle spacing observed in the experiments are very similar to the predictions.

A match of overall heat transfer coefficient between the experiments and simulations was not expected due to the different mass flow rates. A B/Ds ratio of 0.45 can be identified to be the optimal at

enhancing the heat transfer, compared to 0.41 noted in the simulations; this difference was also due to the fact that baffle number can only be varied in whole numbers. The match not only validates the numerical methodology employed, but also confirms CFD to be an efficient tool to assess and design HXs with multiple tube passes provided the grid resolution and boundary conditions are chosen properly. Besides, the study also elucidates use of CFD models for design purposes are beneficial since they are able to identify the source and location of the weakness in design, making it easier for the designer to bring an improvement.

Table 5
Baffle spacing for different baffle configurations tested (Experimental)

No of baffles	**No of baffles**	**4**	**6**	**8**	**10**	**12**	**14**	**16**
Experimental	Baffle spacing B (mm)	209.3	125.6	89.7	69.8	57.1	48.3	N/A
	B/Ds ratio	1.36	0.82	0.58	0.45	0.37	0.31	N/A
Simulation	Baffle spacing B (mm)	385	221	165.3	127	102.4	85.5	73.5
	B/Ds ratio	1.26	0.72	0.54	0.42	0.34	0.28	0.24

Conclusions

The objective of the study was to explore the effect of changing number of baffles on heat transfer and pressure drops for a multiple tube pass HX.

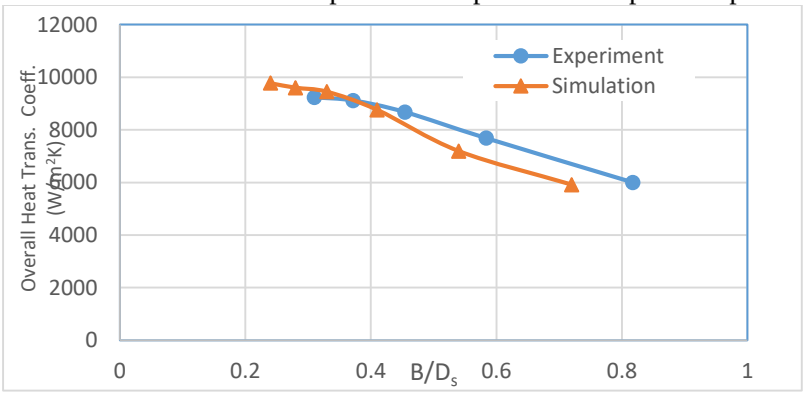

Fig. 9. Comparison of Heat Transfer Coefficient in Experiments and Simulations at different baffle spacing

The study revealed that decrease in inter baffle spacing caused an increase in heat transfer, but the advantage diminishes beyond 10 baffles i.e. an increase in heat transfer of 28.53% for 12 baffles was observed compared to 25.45% for 10 baffles, showing only a 3% further improvement. Pressure drops calculated using the Bell-Delaware method showed a parabolic increase with increase in the baffle number.

A baffle spacing to shell diameter ratio B/D_s of 0.41 was identified to be the optimal for thermohydraulic performance, against an experimentally determined value of 0.45. Thus, for optimal performance, STHXs with B/D_s of 0.4-0.5 should be designed. A much broader range of 0.3-0.6 available in the literature is primarily due to the variance in shell dimensions amongst the different studies, and the fact that baffle number, which controls the B/D_s can only be varied in whole numbers. Agreement between the experimental and numerical investigation elucidates that CFD is an alternative and powerful method for designing better HXs. CFD only indicates a problem in design, it also identifies the source and location of the weakness in design, making it easier to bring improvements. The numerical methodology adopted in this investigation can be used to design industrial HXs for power generation, energy conservation and other applications that incorporate multiple tube passes.

Nomenclature

A	Area of Heat Exchanger, m^2
B	Inter Baffle Spacing, m
B_s	Percentage Baffle Cut
C_{max}	Heat Capacity rate of Maximum Fluid, W/K
C_{min}	Heat Capacity rate of Minimum Fluid, W/K
c_p	Specific heat, J/kgK
D_s	Shell Inside Diameter
HXs	Heat Exchangers
k	Turbulent kinetic energy, m^2/s
m_h	Mass flow rate of hot fluid, kg/s
m_c	Mass flow rate of cold fluid, kg/s
N	Number of Baffles
Np	Number of Tube passes
NTU	Number of Transfer units
p	Pressure, Pa
q	Heat Transfer Rate, kW
q_{max}	Maximum Possible Heat Transfer Rate, kW
T_{hi}	Temperature of hot fluid at inlet, K

T_{ho} Temperature of hot fluid at outlet, K
T_{ci} Temperature of cold fluid at inlet, K
T_{co} Temperature of cold fluid at outlet, K
U Overall Heat Transfer Coefficient, W/m^2K
Greek Symbols
ε Effectiveness of Heat Exchanger

References

Andrews, M. J., & Master, B. I. (2005). Three Dimensional Modeling of a Helixchanger Heat Exchanger using CFD. *Heat Transfer Engineering, 26*(6), 22-31.

Ansys fluent theory guide. (n.d.). Retrieved from www.ansys.com.

Bell, K. J. (1963). *Final Report of the Cooperative Research Program on Shell and Tube Heat Exchangers, bulletin no. 5.* New York: University of Delaware Engineering Experiment Station.

Bergman, T. L., Lavine, A. S., Incropera, F. P., & Dewitt, D. P. (2011). *Fundamentals of Heat and Mass Transfer.* John Wiley & Sons.

Biswas, G., & Eswaran, V. (2002). *Turbulent Flows, Fundamentals, Experiments and Modeling.* CRC Press.

Cao, E. (2010). *Heat transfer in process engineering* (1st ed.). New York, NY, USA: McGraw-Hill Education.

Cengel, Y. A. (2003). *Heat Transfer: A Practical Approach.* McGraw-Hill.

Jain, A., Jain, K. K., & Patel, S. (2015). Comparative study of different CFD models to evaluate Heat Transfer and Flow parameters in STHE. *International Journal of Engineering Sciences and Research Technology,* 536-547.

Jozaei, A. F., Baheri, A., Hafshejani, M. K., Arad, A., & Falavan, A. (2012). Optimization of Baffle Spacing on Heat Transfer, Pressure Drop and Estimated Price in a Shell-and-Tube Heat Exchanger. *World applied Sciences Journal, 18*(12), 1727-1736.

Kakac, S., & Hongtan, L. (2000). *Heat Exchangers: selection, rating and thermal design.* New York (NY): CRC Press LLC.

Kern, D. (1997). *Process Heat Transfer.* New Delhi: Tata McGraw Hill, .

Kottke, H. L. (1999). Analysis of local shellside heat and mass transfer in the shell-and-tube heat exchanger with disc-and-doughnut baffles. *International Journal of Heat and Mass Transfer, 42*(18), 3509-3521.

Liu, J. Y. (2015, September). Numerical investigation on a novel shell-and-tube heat exchanger with plate baffles and experimental validation. *Energy Conversion and Management, 101*, 689-696.

Master, B. I., Chunangad, K. S., & Pushpanathan, V. (2003). Fouling mitigation using helixchanger heat exchangers. *Proceedings of the ECI Conference on Heat Exchanger Fouling and Cleaning: Fundamentals and Applications* (pp. 317-322). Santa Fe, New Mexico, USA: Engineering Conferences International, New York, U.S.A.

Mukherjee, R. (1998). Effectively Design Shell-and-Tube heat exchangers. *Chemical Engineering Progress, 94*, 21-37.

Ozden, E., & Tari, I. (2010). Shell Side CFD Analysis of a small shell-and-tube heat exchanger. *Energy Conversion and Management, 51*, 1004 - 1014.

Pal, E., Kumar, I., Joshi, J., & Maheshwari, N. (2016). CFD simulations of shell-side flow in a shell-and-tube type heat exchanger with and without baffles. *Chemical Engineering Science, 143*, 314-340.

Prithiviraj, M., & Andrews, M. (1998). Three dimensional numerical simulation of shell-and-tube heat exchangers. Part 1: foundation and fluid mechanics. *Numerical Heat Transfer, Part A, 33*, 799 816.

Stehlik, P., Nemcansky, J., Kral, D., & Swanson, L. W. (1994). Comparison of Correction Factors for Shell and Tube Heat Exchangers with Segmented or Helical Baffles. *Heat Transfer Engineering, 15*(1), 55-65.

Sun Y, W. X. (2019). Numerical Investigation and Optimization on Shell Side Performance of A Shell and Tube Heat Exchanger with Inclined Trefoil-Hole Baffles. *Energies, 12*(21), 4138-4160.

Sunden, B. (2007). Computational Fluid Dynamics in Research and Design of Heat Exchangers. *Heat Transfer Engineering, 28*(11), 898–910.

Wang, J. Q., Chen, Q., Chen, G., & Zing, M. (2009). Numerical Investigation on Combine Multiple Shell-Pass Shell and Tube Heat Exchanger wih Continuous Helical Baffles. *Inernational Journal of Heat and Mass Transfer, 52*, 1214-1222.

Wang, J. Q., Chen, Q., Chen, G., & Zing, M. (2009). Numerical InvestIgation on Combine Multiple Shell-Pass Shell and Tube Heat Exchanger wih Continuous Helical Baffles. *Inernational Journal of Heat and Mass Transfer, 52*, 1214-1222.

Williams, P. S., & Knudsen, J. G. (1963). Local rates of heat transfer and pressure losses in the vicinity of annular orifices. *The Canadian Journal of Chemical Engineering, 41*, 56-61.

Xianhe, D., & Songjiu, D. (1998). Investigation of Heat Transfer Enhancement of Roughened Tube Bundles Supported by Ring or Rod Supports. *Heat Transfer Engineering, 19*(2), 21-27.

Yang, J., & Liu, W. (2015). Numerical investigation on a novel shell and tube heat exchanger with plate baffles and experimental validation. *Energy Conversion and Management, 101*, 689-696.

Yang, J., Ma, L., Bock, J., Jacobi, A., & Liu, W. (2014). A Comparison of Four Numerical Modeling Approaches for Enhanced Shell-and-Tube Heat Exchangers with Experimental Validation. *Applied Thermal Engineering, 65*, 369-383.

Yonghua, Y., Yuqi, C., Mergqian, X., Xiaobing, L., Loan, J., & Suyi, H. (2015). Numerical Simulation and Perfomance Improvement for a Small Size Shell and Tube Heat Exchanger with Tre-Foil-Holes Baffles. *Applied Thermal Engineering, 89*, 220-228.

You, Y., Fan, A., Liu, W., & Huang, S. (2012). Thermo-hydraulic characteristics of laminar flow in an enhanced tube with conical strip inserts. *International Journal of Thermal Sciences, 61*, 28-37.

You, Y., Shufang, X., Pan, N., & Deng, Z. (2018). Full Model Simulation of Shellside Thermal Augmentation of Small Heat Exchanger with Two Tube Passes. *Heat Transfer Engineering, 39*(12), 1024-1035.